Electrical Engineering 85 (2003) 129–135 © Springer-Verlag 2003
DOI 10.1007/s00202-003-0158-6

# On the electromagnetic scattering of a chaff cloud

**Z.D. Zaharis, J.N. Sahalos**



**Abstract** Scattering characteristics of a chaff are investigated, using a cloud of wire dipoles. The influence of mutual coupling between the dipoles is taken into account. The cloud is studied in terms of the resonant conditions. Algorithms to specify the stochastic distribution of the dipole positions and orientations are constructed. Finally, the possibility of tracing an obscure target behind the cloud is examined.

**Keywords** Chaff cloud, Dipole cloud, Radar cross-section, Electromagnetic scattering, Target detection

## 1
## Introduction

Chaff clouds, also known as Windows or as Düppel clouds, have been investigated in the past due to great practical interest . As a defensive measure, chaff is quite old but still effective [1]. Compared with other electronic countermeasures, it is relatively quite inexpensive because it comprises metallic or metal-coated fibers. Chaff clouds generate false echoes in search radars or act as decoy targets to confuse radar systems [2]. When the chaff dipoles resonate at radar frequencies, they have maximum radar reflectivity.

The basic difficulty in the study of scattering characteristics comes from the mutual coupling among dipoles. Mutual coupling converts the mathematical analysis of clouds into a non-linear problem. Neglecting mutual coupling, the average backscattering cross section comes from the corresponding one of a single dipole [3], multiplied by the number of dipoles present. The appearance of multiple scattering among the dipoles creates coupling which depends on the number, the direction, and the distance between the dipoles. Mutual coupling must be seriously taken into account in scattering calculations.

*Received: 23 October 2002 / Accepted: 10 January 2003*
*Published online: 26 February 2003*

Z.D. Zaharis, J.N. Sahalos (✉)
Radiocommunications Laboratory, Department of Physics,
Aristotle University of Thessaloniki,
54124 Thessaloniki, Greece
E-mail: sahalos@auth.gr
Tel.: +30-310998161
Fax: +30-310998069

To be as close to reality as possible, the number of chaff dipoles must be the maximum possible. Considering wire dipoles with axial current distribution, the analysis of the cloud can be made using software that implements the method of moments [5]. It is noticed that in any case the number of dipoles is smaller than a typical chaff. However, it is believed that the results can be extended to such a cloud.

Packaging configurations and atmospheric conditions influence the electromagnetic characteristics of a chaff cloud in time. As time passes, the cloud tends to become less dense. In the present study, we assume that time is stopped at regular intervals for which the cloud does not change. In each interval, the backscattering is calculated. This kind of determination of the cross section is actually based upon a static (frozen) model. The static model was tried in the past [3, 9] and found to be useful in practice. Comparisons with experiments [3] have shown acceptable accuracy.

## 2
## Model development

To calculate the scattering characteristics of a chaff cloud, a proper description is needed. The spherical form of the cloud is typical. In this form, the positions are distributed around the center of the cloud at random, following a Gaussian distribution. The center of the cloud is specified at the origin of the coordinate system. The dipole centers are determined by the coordinates $x$, $y$, $z$, and follow Gaussian distribution with normalized probability density functions given by:

$$p(x) = \frac{1}{\sigma_x\sqrt{2\pi}} e^{-\frac{x^2}{2\sigma_x^2}}$$
$$p(y) = \frac{1}{\sigma_y\sqrt{2\pi}} e^{-\frac{y^2}{2\sigma_y^2}} \quad (1)$$
$$p(z) = \frac{1}{\sigma_z\sqrt{2\pi}} e^{-\frac{z^2}{2\sigma_z^2}}$$

$\sigma_x$, $\sigma_y$, $\sigma_z$ are the standard deviations in the three axes respectively. For different $\sigma_x$, $\sigma_y$, $\sigma_z$, clouds of various types are shaped. In the specific case of a spherical cloud, it is $\sigma_x$=$\sigma_y$=$\sigma_z$. Standard deviation determines the extension of the cloud in space (Fig. 1).

Apart from the position, the dipole orientation is also stochastic and is defined by angles $\theta$ and $\phi$ of the spherical coordinate system. Considering the same probability in every direction around the $z$ axis, it can be shown [4] that

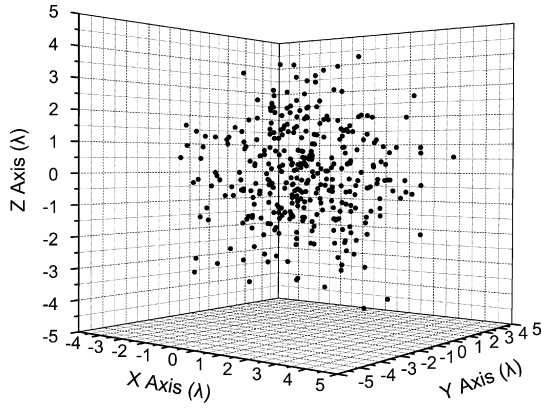


**Fig. 1.** 350 dipole positions of Gaussian distribution with standard deviation $\sigma_x=\sigma_y=\sigma_z=1.5\lambda$

the probability density function of the angle $\phi$ is given by the expression:

$$p(\varphi)=\frac{1}{2\pi} \tag{2}$$

Angle $\theta$ is distributed in the form

$$p(\theta)=\frac{1}{2}\sin\theta \tag{3}$$

Equation (3) implies that the dipoles tend to be located parallel to the $xy$ plane.

Algorithms based on expressions (1), (2) and (3) were constructed to specify the position and the orientation of each dipole in the cloud. It is obvious that the dipoles do not intersect each other.

## 3
## Electromagnetic scattering

Wire dipoles have radii, $a$, much shorter than the wavelength $\lambda$ ($a \ll \lambda$). In addition, the current density follows the axial direction along each dipole.

According to the method of moments [5, 6, 7], the electric current $I(\ell)$ along the dipoles can be evaluated as a linear combination of a set of $N$ expansion functions $F_n(\ell)$, as follows:

$$I(\ell)=\sum_{n=1}^{N} I_n F_n(\ell) \tag{4}$$

$F_n(\ell)$ represent the expansion modes (Fig. 2) and are defined as vectors by

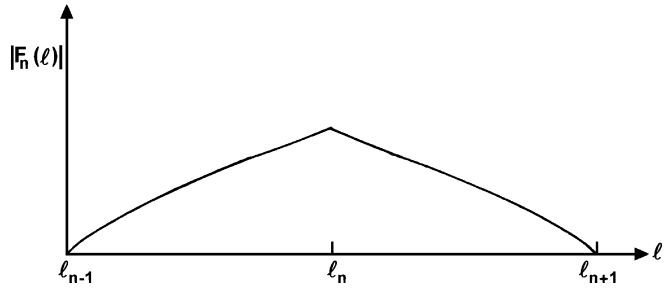


**Fig. 2.** Diagram of the expansion mode amplitude

$$\mathbf{F}_n(\ell)=\begin{cases}\hat{s}_n\dfrac{\sinh\gamma(\ell-\ell_{n-1})}{\sinh\gamma(\ell_n-\ell_{n-1})}, & \ell_{n-1}\le\ell\le\ell_n\\ \hat{s}_n\dfrac{\sinh\gamma(\ell_{n+1}-\ell)}{\sinh\gamma(\ell_{n+1}-\ell_n)}, & \ell_n\le\ell\le\ell_{n+1}\end{cases} \tag{5}$$

where $\hat{s}_n$ is the axial unit vector along each dipole and $\ell_{n-1}$, $\ell_n$, $\ell_{n+1}$ are the positions of three sequential points, among which the $\mathbf{F}_n(\ell)$ is defined. $\gamma$ is the complex propagation constant of the homogeneous ambient material and is defined by

$$\gamma=\alpha+j\beta \tag{6}$$

where $\alpha$ is the attenuation coefficient and

$$\beta=\frac{2\pi}{\lambda} \tag{7}$$

is the wave number.

Using the reaction integral equation [6] and applying (4), a linear system of equations results. In matrix form, it is as follows:

$$\begin{bmatrix} Z_{11} & Z_{12} & \ldots & \ldots & Z_{1N}\\ Z_{21} & Z_{22} & \ldots & \ldots & Z_{2N}\\ \ldots & \ldots & \ldots & \ldots & \ldots\\ \ldots & \ldots & \ldots & \ldots & \ldots\\ Z_{N1} & Z_{N2} & \ldots & \ldots & Z_{NN}\end{bmatrix}\begin{bmatrix} I_1\\ I_2\\ \ldots\\ \ldots\\ I_N\end{bmatrix}=\begin{bmatrix} V_1\\ V_2\\ \ldots\\ \ldots\\ V_N\end{bmatrix} \tag{8}$$

The elements $Z_{mn}$ are the mutual impedances calculated by

$$Z_{mn}=-\int_n \mathbf{E}_m\cdot\mathbf{F}_n\,\mathrm{d}\ell \tag{9}$$

$\mathbf{E}_m$ is the electric field applied by the $m$th expansion mode ($\mathbf{F}_\mathrm{m}$) on the $\mathbf{F}_n$. $I_n$ are the currents at the points that were initially defined on the dipoles, while the elements $V_m$ of the third matrix represent the equivalent voltage excitations. $V_m$ is given by:

$$V_m=\int_m \mathbf{F}_m\cdot\mathbf{E}_i\,\mathrm{d}\ell \tag{10}$$

where $\mathbf{E}_i$ denotes the incident electric field at the position of the $m$th mode.

Using well-known analytical expressions for components $\mathbf{E}_{\theta\mathrm{n}}$ and $\mathbf{E}_{\varphi\mathrm{n}}$ of the expansion mode electric field, the corresponding components of the scattered field can be extracted. These are:

$$\begin{aligned}\mathbf{E}_{\theta s}&=\sum_{n=1}^{N} I_n\mathbf{E}_{\theta n}\\ \mathbf{E}_{\varphi s}&=\sum_{n=1}^{N} I_n\mathbf{E}_{\varphi n}\end{aligned} \tag{11}$$

The echo areas of the cloud can be computed as follows:

$$\sigma_{\theta\theta}=\lim_{r\to\infty}\left(4\pi r^2\mathrm{e}^{2\alpha r}\frac{\mathbf{E}_{\theta s}\cdot\mathbf{E}^*_{\theta s}}{\mathbf{E}_{\theta i}\cdot\mathbf{E}^*_{\theta i}}\right) \tag{12}$$

$$\sigma_{\varphi\theta}=\lim_{r\to\infty}\left(4\pi r^2\mathrm{e}^{2\alpha r}\frac{\mathbf{E}_{\theta s}\cdot\mathbf{E}^*_{\theta s}}{\mathbf{E}_{\varphi i}\cdot\mathbf{E}^*_{\varphi i}}\right) \tag{13}$$

$$\sigma_{\theta\varphi} = \lim_{r\to\infty}\left(4\pi r^2 \mathrm{e}^{2\alpha r}\frac{\mathbf{E}_{\varphi s}\cdot\mathbf{E}^*_{\varphi s}}{\mathbf{E}_{\theta i}\cdot\mathbf{E}^*_{\theta i}}\right) \tag{14}$$

$$\sigma_{\varphi\varphi} = \lim_{r\to\infty}\left(4\pi r^2 \mathrm{e}^{2\alpha r}\frac{\mathbf{E}_{\varphi s}\cdot\mathbf{E}^*_{\varphi s}}{\mathbf{E}_{\varphi i}\cdot\mathbf{E}^*_{\varphi i}}\right) \tag{15}$$

where $\mathbf{E}_{\theta\mathrm{i}}$ and $\mathbf{E}_{\varphi\mathrm{i}}$ are the incident electric field components.

## 4 Results

The scattering characteristics of a spherical cloud of dipoles were studied. The positions and the directions of the dipoles were defined from algorithms, which operate as random number generator functions based on Eqs. (1), (2), and (3). The analysis of the whole process was based on the method of moments.

By taking into account the statistical behavior of the cloud regarding the linear-to-linear backscattering, the echo areas were calculated. According to [3], Borison has shown that the probability density should approach a Rayleigh power curve given by

$$p(\sigma) = \frac{1}{\sigma_{\mathrm{av}}}\mathrm{e}^{-\sigma/\sigma_{\mathrm{av}}} \tag{16}$$

$\sigma_{\mathrm{av}}$ is the average backscattering cross section neglecting mutual coupling between dipoles. $\sigma_{\mathrm{av}}$ must be:

$$\sigma_{\mathrm{av}} = N\sigma_1 \tag{17}$$

where N is the number of dipoles, and $\sigma_1$ is the average cross section of a single dipole.

Given that $\sigma_1=0.15\lambda^2$, for 100 dipoles it is $\sigma_{\mathrm{av}}=15\lambda^2$. Testing several clouds of different standard deviation in the distribution of dipole positions, the normalized probability density distributions versus the linear-to-linear echo area were found (see Figs. 3, 4). The probability distributions were fitted by a Rayleigh power curve. From Fig. 3, one can see that the average echo area of the cloud comes very close to the value of $15\lambda^2$ for clouds of low dipole density. For larger cloud densities (Fig. 4), the average echo area diverts notably from the above-mentioned value. That happens because mutual coupling between dipoles performs a most crucial impact on the backscattering characteristics of the cloud.

The influence of coupling can also be demonstrated by fitting the cumulative probability distribution according to the Rayleigh power curve for two cases of different cloud density (Fig. 5). In Fig. 6, the normalized average linear-to-linear echo area of a 100 dipole cloud versus the average dipole spacing is presented. The echo area starts from low values, whereas the coupling is strong, and increases with small fluctuations up to the value of $15\lambda^2$. Our results extend the corresponding ones of [3] and verify that coupling principally depends on the density of the cloud. For an average spacing of the dipoles of about $0.25\lambda$, coupling reduces the normalized echo area up to −8.5 dB. For average spacing of more than $2\lambda$, the coupling effect is negligible.

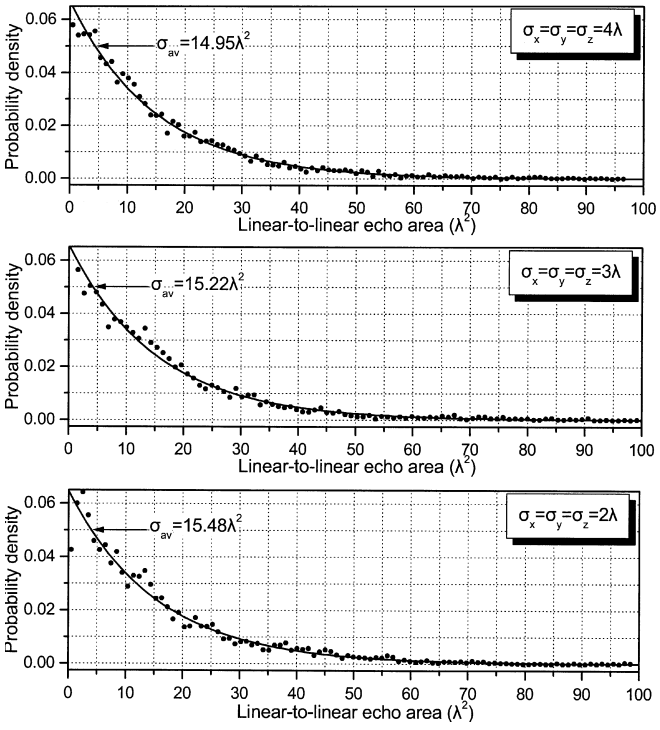


**Fig. 3.** Normalized probability density distributions of the linear-to-linear echo area for standard deviation $4\lambda$, $3\lambda$, and $2\lambda$ in the distribution of dipole positions

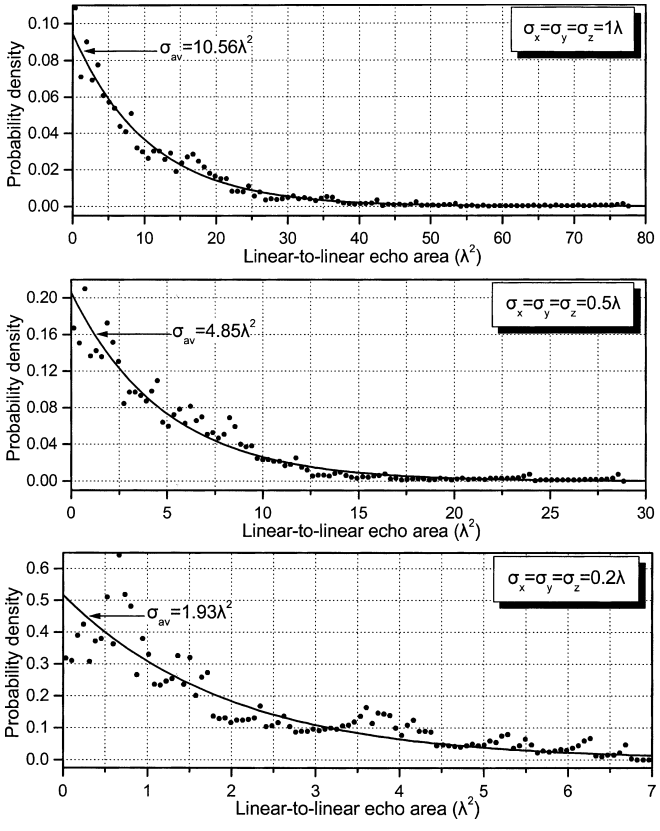


**Fig. 4.** Normalized probability density distributions of the linear-to-linear echo area for standard deviation $1\lambda$, $0.5\lambda$, and $0.2\lambda$ in the distribution of dipole positions

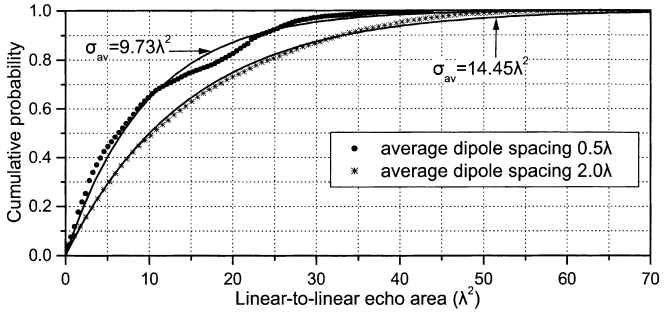




**Fig. 5.** Cumulative probability distributions of the linear-to-linear echo area for average dipole spacing $0.5\lambda$ and $2\lambda$

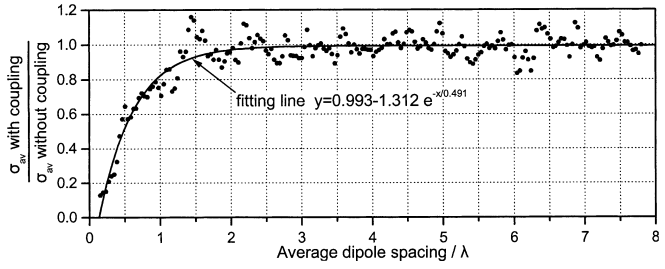


**Fig. 6.** Normalized average linear-to-linear echo area of an 100 dipole spherical cloud as a function of the average dipole spacing

Scattering characteristics are strongly related to the resonant condition of the dipoles [8]. In the frequency where the dipoles are close to $\lambda/2$ in length, the resonant condition maximizes the dipole current. Consequently, the cloud scattering increases and maximizes the echo areas. Figure 7 shows the variation in the echo area $\sigma_{\theta\theta}$ as a function of the dipole length. Results were acquired for a 100 dipole cloud with a Gaussian density distribution of standard deviation $\sigma_x=\sigma_y=\sigma_z=2\lambda_0$ in the dipole positions, while the dipoles were chosen equal to $0.475\lambda_0$ in length ($\lambda_0$ is the resonant wavelength). It is obvious that the echo area is maximized around the first resonance of the dipoles, while few maxima of lower values appear around the higher-order resonance. It is noticed that $\sigma_{\theta\theta}$ has been taken at the angle $\phi=0°$. If we evaluate the average $\bar{\sigma}_{\theta\theta}$ by taking into account all $\sigma_{\theta\theta}(\phi)$, we have a smoother response. Figure 7 presents $\bar{\sigma}_{\theta\theta}$, which is also maximized around the first resonance of the dipoles.

It is interesting to examine the ability of a 100 dipole cloud to hide a target. The target is positioned either above the cloud (barrier configuration) towards $\theta=0°$ or inside it (side configuration). The cloud continues to have a Gaussian distribution in the dipole positions with $\sigma_x=\sigma_y=\sigma_z=2\lambda_0$. The target is a square conducting plate parallel to the xy plane. The echo area is found for different dimensions and different positions of the target in space.

Figures 8, 9, 10, and 11 present the normalized average linear-to-linear echo area of a target $1\lambda_0\times1\lambda_0$ plus and minus the echo area of the cloud, as well as the normalized average linear-to-linear echo area of the ensemble. The target with distance $0\lambda_0$ (see Fig. 8) is at the center of the cloud. The cloud has a radius of about $r=5.7\lambda_0$. Obviously,

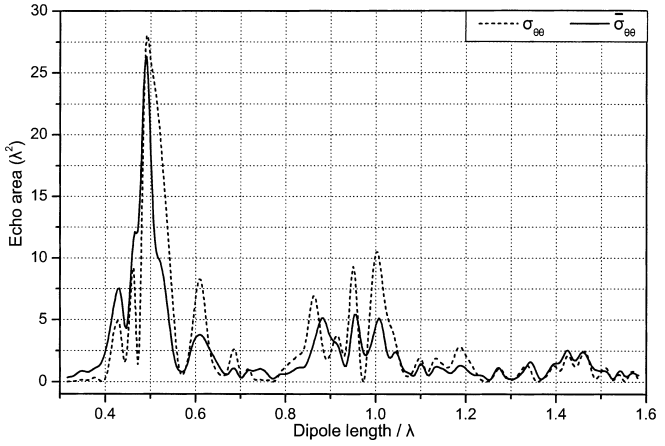


**Fig. 7.** Echo areas $\sigma_{\theta\theta}$ and $\bar{\sigma}_{\theta\theta}$ for a 100 dipole spherical cloud as a function of the dipole length

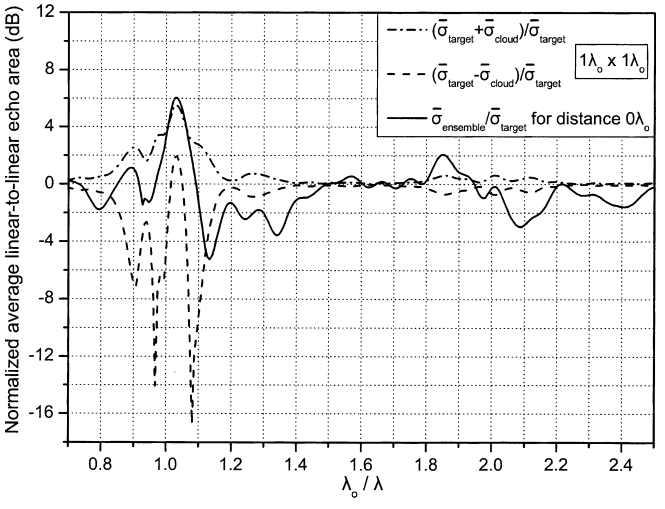


**Fig. 8.** Normalized average linear-to-linear echo area for a $1\lambda_0\times1\lambda_0$ target at a distance of $0\lambda_0$ from a spherical cloud of 100 dipoles and $2\lambda_0$ standard deviation of the dipole positions

the target with distance $10\lambda_0$ is in barrier configuration (Fig. 11). In the side configurations (Figs. 8, 9, 10), it is shown that around the resonant length of the dipoles there is a ~6 dB increase in the echo area of the ensemble. Far from the resonance, the difference between the ensemble and the target echo area is much smaller. For the barrier configuration (Fig. 11), we have a significant oscillation of the echo area independently of the dipole length. Obviously, except for the resonant frequency, it seems that the cloud is not an accepted hiding place.

To secure the above conclusion, a target with dimensions $4\lambda_0\times4\lambda_0$ was used. Figure 12 presents the echo areas for different distances between the center of the cloud and the target. Here the coupling gives conditions of decreasing echo area at the resonant frequency. This is something which was also observed in [9] for the same target and a 50 dipole cloud. Since there is much different behavior between the $1\lambda_0\times1\lambda_0$ and the $4\lambda_0\times4\lambda_0$ target, two other targets of $2\lambda_0\times2\lambda_0$ and $3\lambda_0\times3\lambda_0$ were studied. Figures 13 and 14 present the echo area for the above two cases. It is obvious

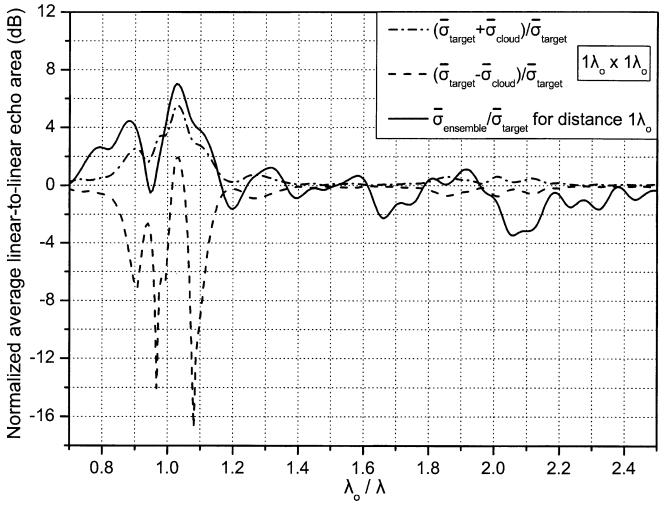


**Fig. 9.** Normalized average linear-to-linear echo area for a $1\lambda_0 \times 1\lambda_0$ target at a distance of $1\lambda_0$ from a spherical cloud of 100 dipoles and $2\lambda_0$ standard deviation of the dipole positions

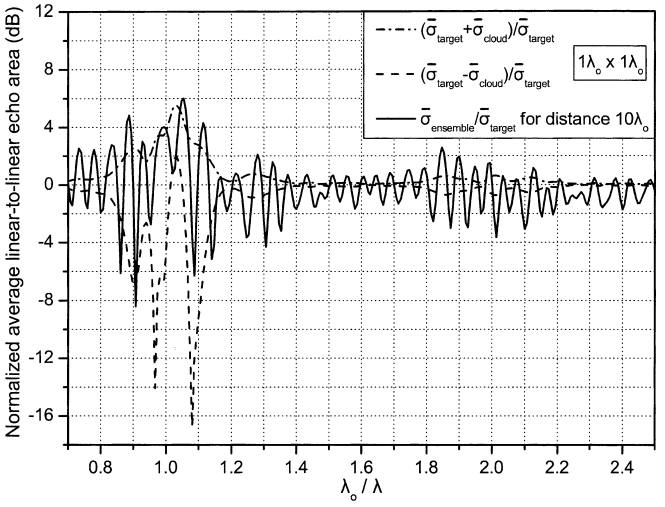


**Fig. 11.** Normalized average linear-to-linear echo area for a $1\lambda_0 \times 1\lambda_0$ target at a distance of $10\lambda_0$ from a spherical cloud of 100 dipoles and $2\lambda_0$ standard deviation of the dipole positions

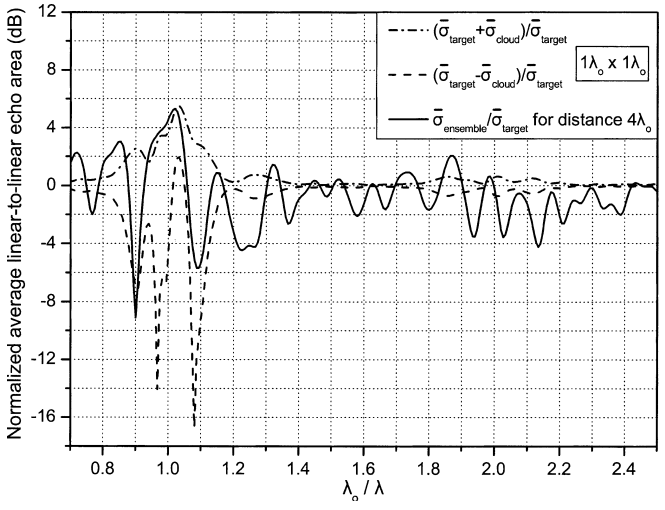


**Fig. 10.** Normalized average linear-to-linear echo area for a $1\lambda_0 \times 1\lambda_0$ target at a distance of $4\lambda_0$ from a spherical cloud of 100 dipoles and $2\lambda_0$ standard deviation of the dipole positions

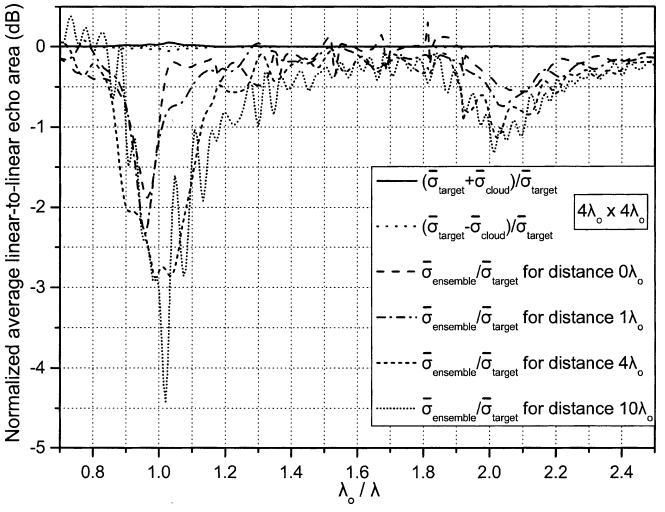


**Fig. 12.** Normalized average linear-to-linear echo area for a $4\lambda_0 \times 4\lambda_0$ target at several distances from a spherical cloud of 100 dipoles and $2\lambda_0$ standard deviation of the dipole positions

from the figures that, at resonance, the coupling conditions increase the ensemble relative echo area as the target decreases.

At resonance and for a target $1\lambda_0 \times 1\lambda_0$, it could be interesting to see the backscattering as a function of the observation direction. The target is at the center of the 100 dipole cloud. Figure 15 presents the average echo area $\bar{\sigma}_{\varphi\varphi}$ in the presence and in the absence of the target over the range of angle $\theta$ from 90° to 180°. $\bar{\sigma}_{\varphi\varphi}$ was calculated by taking into account all $\sigma_{\phi\phi}(\phi)$. The diagram does not indicate any significant difference in the scattering characteristics for a certain angle $\theta$.

To hide the target, the cloud density must obviously increase. For a Gaussian distribution in the dipole positions with $\sigma_x=\sigma_y=\sigma_z=0.25\lambda_0$, the results appear to be different from before. An ensemble comprising a $1\lambda_0 \times 1\lambda_0$ square conducting target positioned parallel to the $xy$ plane behind a 100 dipole cloud has an echo area less than that given by the target itself. Figure 16 presents the normalized average echo area for two target distances from the cloud center. In both cases, the echo area of the ensemble is 4 dB less than the echo area of the target at the resonant frequency and much less at other frequencies. This is something very important because the hiding of the target is obvious. It seems that if one takes into account the coupling effect and increases the density of the cloud, the value of the radar cross section (RCS) of the ensemble decreases by an appreciable percentage.

Finally, the echo area was calculated in the time domain. The same cloud as before with 100 dipoles and a $4\lambda_0 \times 4\lambda_0$ target at a distance of $10\lambda_0$ from the center of the cloud was studied. A radiofrequency (RF) pulse of 1.2 GHz center frequency and 20 ns duration was transmitted normally to the target. In one case, the bandwidth of the system was 300 MHz and in the other was 100 MHz. In both cases, the difference between the echo areas of the

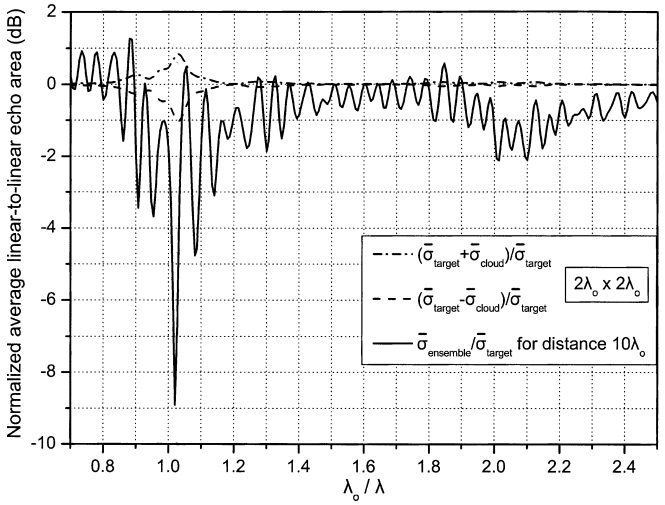


**Fig. 13.** Normalized average linear-to-linear echo area for a $2\lambda_0 \times 2\lambda_0$ target at a distance of $10\lambda_0$ from a spherical cloud of 100 dipoles and $2\lambda_0$ standard deviation of the dipole positions

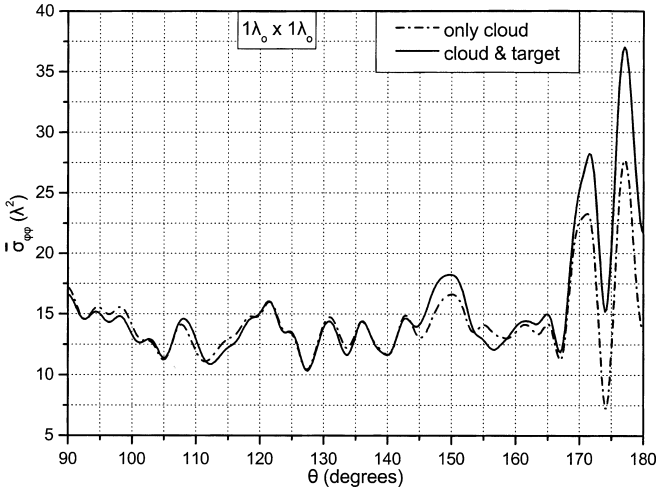


**Fig. 15.** Variation in $\bar{\sigma}_{\varphi\varphi}$ of a 100 dipole spherical cloud vs the observation direction, in the presence and the absence of a $1\lambda_0 \times 1\lambda_0$ target positioned at the center of the cloud

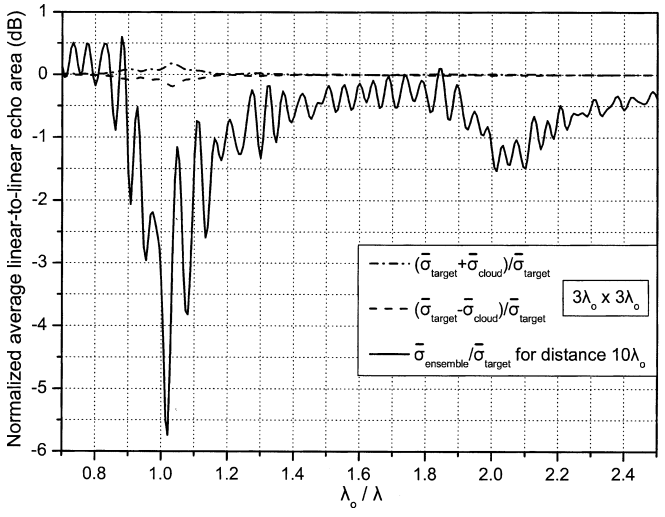


**Fig. 14.** Normalized average linear-to-linear echo area for a $3\lambda_0 \times 3\lambda_0$ target at a distance of $10\lambda_0$ from a spherical cloud of 100 dipoles and $2\lambda_0$ standard deviation of the dipole positions

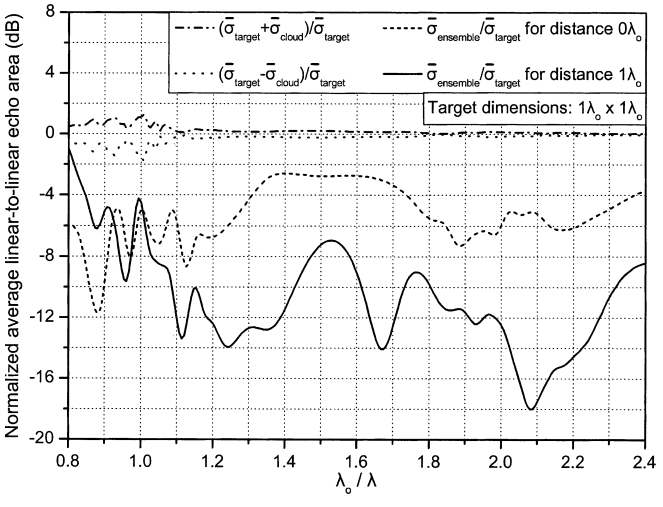


**Fig. 16.** Normalized average linear-to-linear echo area for a $1\lambda_0 \times 1\lambda_0$ target at distances of $0\lambda_0$ and $1\lambda_0$ from a spherical cloud of 100 dipoles and $0.25\lambda_0$ standard deviation of the dipole positions

target and the ensemble was found to be in the appearance of a tail in the responding signal (see Figs. 17 and 18). Obviously, that comes from the reflection between the target and the cloud. It is noticed that the same effect was observed in [9] for 50 dipoles and the same target.

In practice, chaff is a dense cloud with approximately cylindrical or ellipsoidal shape. As the chaff falls, it has a shape in which the horizontal distribution dominates. A reasonable presentation of the chaff could be given if $\sigma_x \neq \sigma_y \neq \sigma_z$. Figure 19 shows the $\sigma_{av}$ for $\sigma_x=2\lambda$, $\sigma_y=1\lambda$ and variable values for $\sigma_z$. It appears that the average RCS decreases as the vertical distribution decreases. This is important, because it turns out that the value $15\lambda^2$ is true only for the spherical symmetry.

Some notations could be eventually given for the polarization of the chaff. As the chaff falls, there is a gradual separation into two clouds. One has predominantly a horizontal polarization and the other a vertical polarization. The vertically polarized dipoles fall faster and their layer is under the horizontally polarized layer.

Our study is related mainly to the self-protection of aircraft. However, for naval ships, the above can be made similarly except that the RCS is larger, and the timing and implementation of the naval mission is more difficult. Also, due to the proximity of the sea to the chaff (~200 m above the surface of the sea), multipath effects must be taken into account, and vertical polarization plays a dominant role.

## 5 Conclusions

The scattering characteristics of a dipole cloud were presented. The method of moments was applied and the mutual coupling of the dipoles was verified. The dependence of the echo area for various densities of the cloud

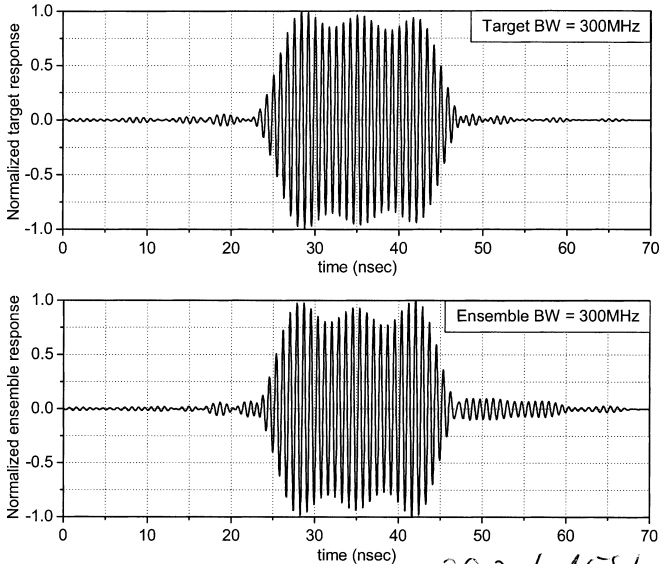


**Fig. 17.** Time domain response of a $4\lambda_0 \times 4\lambda_0$ target, in the presence and the absence of a 100 dipole spherical cloud for a RF pulse with 300 MHz bandwidth

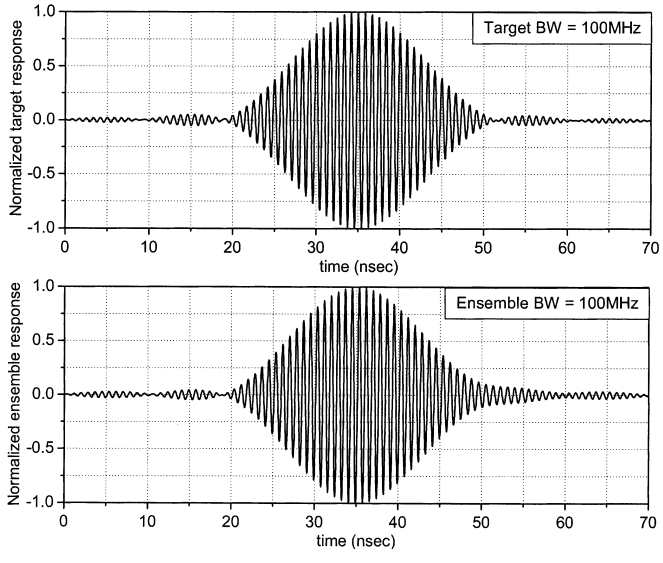


**Fig. 18.** Time domain response of a $4\lambda_0 \times 4\lambda_0$ target, in the presence and the absence of a 100 dipole spherical cloud for a RF pulse with 100 MHz bandwidth

upon the radiation wavelength and the observation angle was discussed.

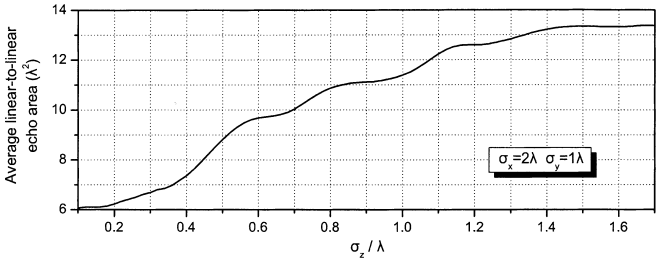


**Fig. 19.** Average linear-to-linear echo area of a 100 dipole ellipsoidal cloud vs the $\sigma_z$ standard deviation of the dipole positions



The important issue for the insertion of a chaff (Düppel) cloud as a hiding place for a target was studied. The effect of the relative position between the cloud and the target was analyzed. Also, the size of the target was taken into account. Finally, the time domain response of a RF pulse incident on the target hidden by the chaff cloud was obtained.

From the analysis, it was found that a Düppel cloud can hide a target at the dipole resonant frequency and for relatively small targets. Otherwise, the echo area of the ensemble is nearly the same as that of the target. At the resonant frequency, different echo areas of the ensemble and the target were found separately.

Finally, in the time domain, the response of a pulse is similar for the ensemble and the target. The only new characteristic that is observed is the appearance of a tail, which comes from the multiple reflections between the cloud and the target.

## References

1. Nathanson FE (1991) Radar design principles: signal processing and the environment. In: Nathanson FE, Reilly JP (eds) Atmospheric effects, weather and chaff, 2nd edn. McGraw-Hill, New York, pp 215–268
2. James RJ (1989) A history of radar. IEE Rev 35:343–349
3. Wickliff RG, Garbacz RJ (1974) The average backscattering cross section of clouds of randomized resonant dipoles. IEEE Trans Antennas Propag 22: 503–505
4. Papoulis A (1991) Probability, random variables, and stochastic processes, 3rd edn. McGraw-Hill, New York
5. Harrington RF (1968) Field computation by moment methods. Macmillan, New York
6. Moore J, Pizer R (1984) Moment methods in electromagnetics, techniques and applications. Research Studies Press, London
7. Hansen RC (1990) Moment methods in antennas and scattering. Artech House, Boston
8. Butters BCF (1982) Chaff. IEE Proc F 129:197–201
9. Las-Heras F, Jambrina JLF (1991) Some results of the scattering of simple conducting bodies in the vicinity of a cloud of dipoles. IEEE Antennas Prop Soc Int Symp Dige 1:26–29